

# Effects of variable anisotropic-strain on the emission of neutral excitons confined in epitaxial quantum dots

J. D. Plumhof<sup>1\*</sup>, V. Křápek<sup>2</sup>, F. Ding<sup>1,3</sup>, K. D. Jöns<sup>4</sup>, R. Hafenbrak<sup>4</sup>, P.

Klenovský<sup>2</sup>, A. Herklotz<sup>5</sup>, K. Dörr<sup>5</sup>, P. Michler<sup>4</sup>, A. Rastelli<sup>1†</sup>, and O. G. Schmidt<sup>1</sup>

<sup>1</sup> *Institute for Integrative Nanosciences, IFW Dresden, Helmholtzstr. 20, D-01069 Dresden, Germany*

<sup>2</sup> *Institute of Condensed Matter Physics, Masaryk University, Kotlářská 2, 61137 Brno, Czech Republic*

<sup>3</sup> *Key Laboratory of Semiconductor Materials Science, Institute of Semiconductors, Chinese Academy of Sciences, Beijing 100083, China*

<sup>4</sup> *Institut für Halbleiteroptik und Funktionelle Grenzflächen,*

*University of Stuttgart, Allmandring 3, 70569 Stuttgart, Germany and*

<sup>5</sup> *Institute for Metallic Materials, IFW Dresden, Helmholtzstr. 20, D-01069 Dresden, Germany*

(Dated: February 15, 2022)

We study the effect of elastic anisotropic biaxial strain on the light emitted by neutral excitons confined in different kinds of semiconductor quantum dots (QDs). We find that the light polarization rotates by up to  $\sim 80^\circ$  and the excitonic fine structure splitting varies by several tens of  $\mu\text{eV}$ s as the strain is varied. By means of a continuum model we mainly ascribe the observed effects to substantial changes of the hole wave function. These results show that strain-fields of a few  $\%$  magnitude are sufficient to dramatically modify the electronic structure of QDs.

Semiconductor quantum dots (QDs) obtained by epitaxial growth are receiving much attention because of their potential use as building blocks for quantum information processing and communication devices [1–7]. QDs confine the motion of charge carriers in three-dimensions and are thus referred to as artificial atoms. Similar to real atoms, external electric and magnetic fields can be used to manipulate the properties of bound states in QDs [8–12]. In addition, the solid-state character of QDs allows for engineering methods which are not available for atoms. Dynamic stress fields [13–16] represent an example, whose wide potential is only recently being recognized [17, 18].

The structural properties of QDs (crystal structure, material composition, shape and size) mainly determine their electronic and optical properties. In particular, the emission of neutral excitons confined in QDs with symmetry lower than  $D_{2d}$  is typically split by several tens of  $\mu\text{eV}$  because of the anisotropic electron-hole exchange interaction [9, 19, 20]. This broken degeneracy of the bright excitonic states, referred to as fine structure splitting (FSS) prevents the use of QDs as sources of entangled photon pairs on demand [4–7, 21]. External electric or magnetic fields have been applied to restore the QD symmetry and achieve FSS values comparable to the radiative linewidth [10, 11, 13]. Seidl *et al.* [14] showed that also uniaxial strain can in principle be used to reduce the excitonic FSS. Due to the limited tuning range available, it has however remained unclear whether strain is suitable to reach sufficiently low values of FSS [5], and what the mechanisms behind the observed FSS changes are.

Recently it was predicted, based on atomistic model simulations for InGaAs/GaAs QDs [18], that anisotropic stress acting on QDs leads to an anticrossing of the bright excitonic

states. Thereby, the magnitude and phase of the mixing of the bright excitonic states are modified which results in a change of the FSS and in a rotation of the linear polarization of the emitted photons [17]. Here we present a detailed experimental proof of this effect and explain its origin by using a continuum model based on 8-band k-p and configuration interaction theory.

The measurements are performed on two different samples grown by solid-source molecular beam epitaxy (MBE). The active structures consist of QDs embedded in thin membranes, which are released from the underlying substrate and transferred onto a piezoelectric actuator [15, 22]. The first membrane sample, with total thickness of about 150 nm, contains GaAs/AlGaAs QDs [23] and quantum well (QW) potential fluctuations (QWPFs) [19, 23]. The latter, which are produced by local thickness or alloy fluctuations in a narrow QW, confine the carriers in all three dimensions and act as QDs with low confinement potential. The second sample contains standard InGaAs/GaAs QDs embedded in 200 nm thick membranes [24]).

The external stress is applied using a piezoelectric  $[\text{Pb}(\text{Mg}_{1/3}\text{Nb}_{2/3}\text{O}_3)_{0.72} - [\text{PbTiO}_3]_{0.28}$  (PMN-PT) crystal. By applying a voltage  $V$  between the front and the back surface of the crystal [i.e. along the  $x$  axis in Fig. 1(b)] the side faces, such as the top  $x - y$  plane, expand (or contract) parallel to the direction of the electric field  $F$ , for positive (negative) applied voltage. Simultaneously, the side faces contract (or expand) perpendicular to the electric field [i.e. along the  $y$  axis in Fig. 1(b)]. We denote the strain parallel to the  $x$  and  $y$  axes as  $\varepsilon$  and  $\varepsilon_\perp$ , respectively. The relation between these strain components is  $\varepsilon_\perp \approx -0.7 \times \varepsilon$  (see Ref. 25). By placing membranes with QDs on the side faces of the PMN-PT we can thus apply strongly anisotropic biaxial stress on the QDs. According to previous results [15, 22], we expect values of  $\varepsilon$  of the order of a few  $\%$  in the explored range of the electric field  $F$ .

Photoluminescence (PL) spectroscopy measurements are performed at a temperature of 8 K in a standard micro-PL

<sup>\*</sup>)Electronic mail: j.d.plumhof@ifw-dresden.de

<sup>†</sup>)Electronic mail: a.rastelli@ifw-dresden.de

setup with a spectral resolution of about  $70 \mu\text{eV}$ . The linear polarization of the luminescence is analyzed by combining a rotatable achromatic half-wave plate and a fixed linear polarizer [24].

Figure 1(a) shows a color-coded PL-intensity map for a neutral exciton (X) confined in a GaAs/AlGaAs QWPF as a function of the emission energy and polarization angle for different values of the electric field  $F$  applied to the PMN-PT (panels 1 to 4:  $F=33, 10, -6.6$  and  $-20 \text{ kV/cm}$ ). In this membrane the electric field direction forms an angle of about  $20^\circ$  with the  $[1\bar{1}0]$  GaAs crystal direction. The polarization dependent periodic energy shift (wavy pattern) observed in PL is ascribed to the excitonic FSS (see Ref. 23).

Two striking features clearly emerge from Fig. 1(a): (i) The polarization direction of the excitonic emission, related to the phase of the wavy pattern, rotates by more than  $60^\circ$  when  $F$  is changed from 33 to  $-20 \text{ kV/cm}$  (see dotted lines); (ii) The magnitude of the FSS, i.e. the amplitude of the oscillations of the wavy patterns, first decreases and then increases with decreasing electric field. To extract quantitative information from the data, we first fit the peak position with a single Lorentzian curve at each polarization angle. The obtained relation of peak position vs polarization angle is then fitted by a sine function to estimate both the magnitude of the FSS and the polarization of the X transitions with respect to the field direction [ $x$  axis in Fig. 1(b)]. The resolution in the determination of the FSS with this procedure is around  $2.5 \mu\text{eV}$  [26].

Figure 1(c)-(e) shows polar plots of the relative peak positions  $\Delta E$  extracted from Fig. 1(a) after subtraction of the average emission energy  $E(F)$  measured for different values of  $F$ . The data, which are averaged over two periods of the polarization-resolved measurements (from  $0^\circ$  to  $360^\circ$  and from  $360^\circ$  to  $720^\circ$ ), clearly show the strain-induced changes both in polarization direction and FSS. Figure 1(f) shows the orientation of the linear polarization of the high energy component of X (with respect to the direction of  $F$ ) as a function of  $E(F)$ . Figure 1(g) shows the corresponding behavior of the FSS. When moving from low to high emission energies, i.e. from tensile to compressive strain along  $x$ , the FSS goes through a broad minimum before increasing again. The maximum observed change of the FSS for this QWPF is about  $50 \mu\text{eV}$ . Concerning the polarization direction we observe that: (i) It shows oscillations superimposed to a smooth decrease when the FSS is minimum; (ii) It appears to saturate with increasing FSS and, more precisely, it is aligned parallel to  $F$  for strong compression (point 4). By repeating similar measurements on different QWPFs we consistently observe the same qualitative behavior: the polarization rotation mainly occurs in correspondence to the minimum of the FSS. Interestingly, the minimum value of the FSS varies from one QWPF to another. Examples where the minimum FSS reaches values below about  $5 \mu\text{eV}$  are presented in Fig. 2(d) and in the supplementary information [24].

In order to test whether the effects observed for GaAs/AlGaAs QWPFs occur also for other QD structures, we have performed similar experiments with GaAs/AlGaAs

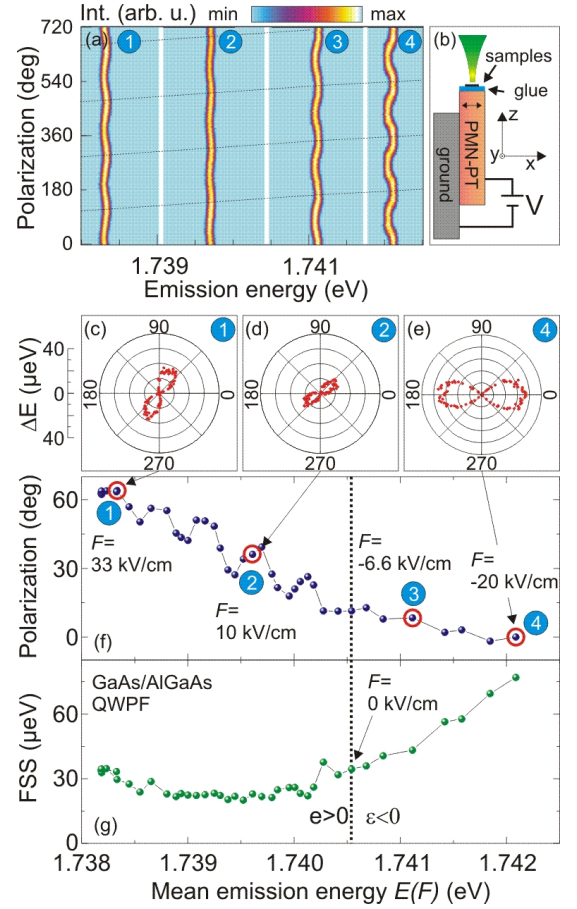


FIG. 1: (Color online) Behavior of a neutral exciton confined in a GaAs/AlGaAs QWPF under anisotropic biaxial stress. (a) Color-coded PL intensity vs polarization angle and energy for different values of electric fields applied to the piezoelectric actuator [the field values for the panels 1 to 4 are indicated in (f)]. The dashed lines are guides to the eye showing the rotation of the polarization direction. The  $x$  direction in (b) corresponds to polarization angles of  $0, 180, 360, 540$  and  $720$  degrees and coincides with the polarization direction of the high-energy component at  $F = -20 \text{ kV/cm}$  (panel 4). (b) Sketch of the device consisting of a membrane (sample) glued on a side of a PMN-PT crystal. (c, d, e) Polarization dependence in polar coordinates of the relative emission energy for panels 1, 2 and 4 of (a). The mean emission energy  $E(F)$  for each value of  $F$  is subtracted. (f) Polarization angle of the high-energy component of X with respect to the direction of the electric field vs  $E(F)$ . The dots marked by red circles correspond to the data shown in (a). (g) FSS vs average emission energy.

QDs, and InGaAs/GaAs QDs (see Fig. 2). For compressive strain, the emission energy of the GaAs/AlGaAs QD presented in Fig. 2(a) and (b) blue shifts similar to the QWPFs, whereas the emission energy of the presented InGaAs/GaAs QD [Fig. 2 (c) and (d)] red shifts. In spite of the very different structural properties and behavior of the emission energy under anisotropic strain, we find that the excitonic behavior of the two different types of QDs is qualitatively the same as that observed for the GaAs/AlGaAs QWPFs: we observe a clear polarization rotation of the emitted light (by  $79^\circ$  for the

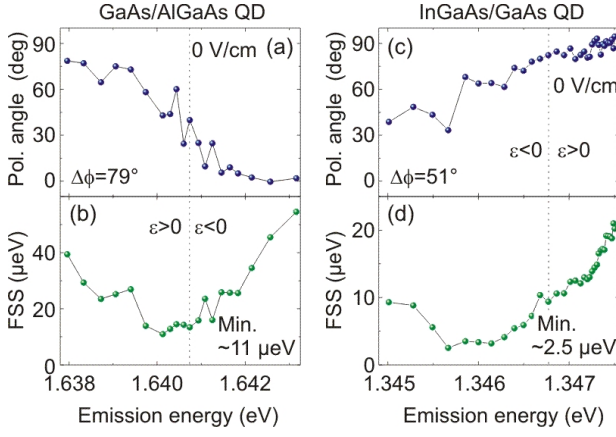


FIG. 2: (Color online) (a,b) Polarization and FSS behavior of a GaAs/AlGaAs QD and (c,d) of an InGaAs/GaAs QD. The polarization angle  $\phi$  is defined as the angle of the higher energetic emission line with respect to the x direction in Fig. 1(b). For both QDs shown here the x direction roughly corresponds to the  $[1\bar{1}0]$  direction of the GaAs-membrane.

GaAs/AlGaAs QD and by  $51^\circ$  for the InGaAs/GaAs QD [see Fig. 2 (a) and (c)]. Simultaneously, the FSS is tuned in a range of  $\sim 70 \mu\text{eV}$  for the GaAs QD and  $\sim 25 \mu\text{eV}$  for the InGaAs QD [see Fig. 2 (b) and (d)]. Furthermore, we observe that the rotation of the polarization mainly takes place when the FSS reaches its minimum value. As in the case of the QWPF presented in Fig. 1, significant fluctuations of the polarization angle are observed in correspondence to the minimum of the FSS.

To explain the physical origin of the dramatic changes in the emission of the neutral excitons, we calculate the excitonic FSS of model dots by combining the eight-band k-p model and the configuration interaction method following the approach described in Refs. 23, 27, 28. Strain is introduced via the Pikus-Bir Hamiltonian [29]. In the model we consider a semi-ellipsoidal GaAs/AlGaAs QD with composition equal to the nominal one used in the experiment. The main axis  $\varepsilon$  of the anisotropic biaxial strain [x axis in Fig. 1(b)] coincides with the  $[1\bar{1}0]$  GaAs crystal direction and we assume  $\varepsilon_\perp \approx -0.7 \times \varepsilon$  [see insets in Fig. 3(b)]. The main axis of the QD forms an angle  $\alpha$  with respect to the  $[110]$  direction [see right inset in Fig. 3(a)] [24].

Figures 3(a) and (b) show, for different values of  $\alpha$ , the calculated polarization angle and the FSS as a function of  $\varepsilon$ , respectively. We begin with the ideal situation of a QD elongated along the  $[110]$  crystal direction ( $\alpha=0$ ). For zero strain, the QD has a FSS of  $33 \mu\text{eV}$ , which is in good agreement with typical observed values. When the QD is stretched, both exciton transitions remain linearly polarized and perpendicular to each other (not shown) and the FSS varies in a wide range [see Fig. 3(b)]. For a strain  $\varepsilon$  of  $0.086 \%$  the FSS reaches its minimum value below  $0.4 \mu\text{eV}$ . The polarization direction of the high energy component, shown in Fig. 3(a), is perpendicular to the elongation direction of the QD for strains below  $0.086 \%$  and abruptly changes by  $90$  degrees for higher

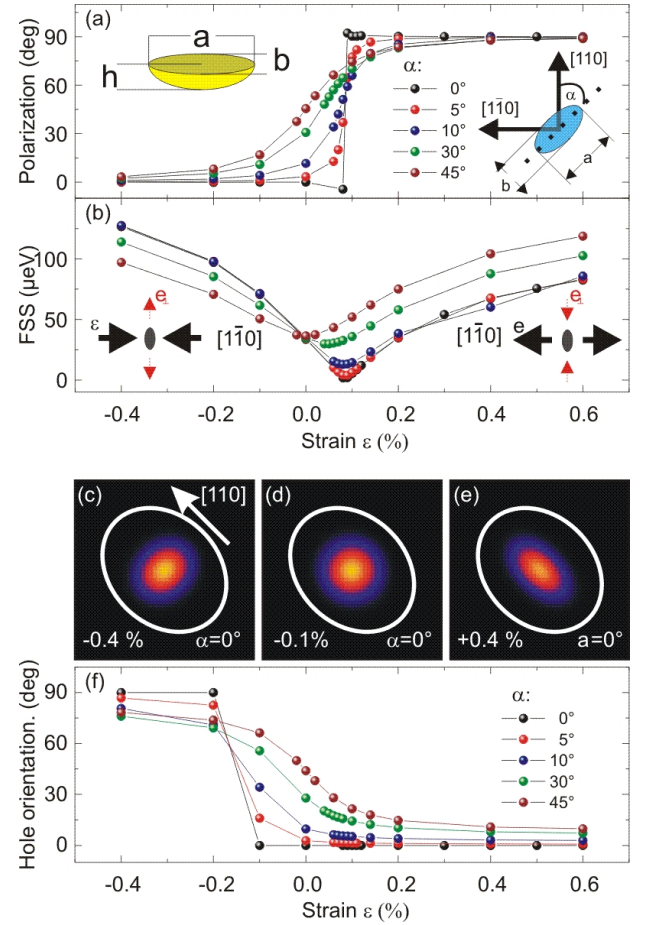


FIG. 3: (Color online) Theoretical study of the influence of anisotropic biaxial strain on the light emitted by an exciton in model GaAs/AlGaAs QDs. The left inset in (a) shows the shape of the artificial structure. (a) Polarization of the high energy excitonic component with respect to the x direction ( $[1\bar{1}0]$ ) in Fig. 2(b) for different values of  $\alpha$  (i.e. angle of the elongation direction with respect to the  $[110]$  crystal direction, see right inset). (b) Corresponding values of the FSS, the left (right) inset displays the direction of the applied stress for compressive (tensile) strains  $\varepsilon$ . (c)-(e) Density map of the hole wave function for a QD with  $\alpha=0$ , for different strain values. The white ellipse indicates the shape of the QD. (f) Orientation of the hole wave function with respect to the  $[110]$  direction vs strain. See text for more details.

strains.

For increasing  $\alpha$ , the polarization direction varies in a wider range of strain values, i.e. it rotates smoothly as a function of strain as shown in Fig. 3(a). Correspondingly, the minimum of the FSS becomes increasingly broad and the reached minimum value increases with increasing  $\alpha$ . We also note that at zero strain the polarization angle is determined by the orientation of the dot. As the strain increases, the structural orientation becomes less important and the polarization angle is determined mostly by the magnitude and direction of the strain, yielding similar values for all dot orientations. This behavior is also observed in the experiments: for the largest available strains, and away from the FSS minimum, anisotropic biax-

ial stress allows us to orient the polarization direction parallel/perpendicular to the strain direction in a predictable way [see Figs. 1(a)-(e)]. Finally we note that similar results are obtained when the direction of the strain direction is changed and the QD is kept fixed instead of rotating the QD shape with respect to the crystal direction as discussed here [24].

Although it is difficult to ascribe the observed strain-induced changes of the FSS to a single effect, we inspected the single particle states and found that small strains produce relevant changes on the hole wave function, while their effect on the electron wave function is much weaker. In particular we find that: (i) The proportion of the light hole band in the hole state is substantially increased (e.g. from 0.6 % at  $\varepsilon=0$  % to 11 % at  $\varepsilon=0.2$  % for  $\alpha=0$ ); (ii) The hole wave function changes in shape and orientation, as illustrated in Fig. 3(c)-(e) for  $\alpha=0$ . In general, for finite values of  $\alpha$ , the elongation direction of holes rotates by up to  $90^\circ$ , as shown in Fig. 3(f). At the same time the electron wave function rotates by  $< 7^\circ$  (not shown).

These effects are a consequence of the non-diagonal terms in the Pikus-Bir Hamiltonian, which enhance the mixing of the heavy hole band with other bands (in particular, the light hole band) and modify the effective mass causing its pronounced anisotropy along the principal stress axes  $[110]$  and  $[\bar{1}\bar{1}0]$ . The smooth rotation of the hole wave function observed for finite values of  $\alpha$  [see Fig. 3(f)], which is analogous to the behavior observed for the polarization direction [see Fig. 3(a)], is due to the joined influence of the structural anisotropy (elongation of the QD) and the anisotropy of the effective mass, which tends to elongate the wave functions along the  $[110]$  or  $[\bar{1}\bar{1}0]$  direction depending on the sign of the applied strain. We note that the effects of the strain induced band edge shift and the created piezoelectric potential on the FSS are negligible. Both effects are comparably small (below 10 meV, for  $\varepsilon=0.2$  %) and do not affect the lateral anisotropy of the wave functions.

In spite of the simplicity of the model QD shape, the presented continuum model is able, for finite values of  $\alpha$ , to account for all of the experimental observations apart from the fluctuations in polarization angle observed in Figs. 1(f) and 2(a),(c). We tentatively ascribe the latter to peculiarities of the shape and composition profiles of real QDs. We thus conclude that atomistic models [17, 18] are not strictly required to explore the main effects produced by stress on the FSS and polarization angle of the excitonic states of QDs, especially in view of the uncertainties in the structural parameters of real QDs.

In conclusion, we have reported on the effects of anisotropic biaxial stress on the emission of neutral excitons confined in single semiconductor QDs. We have shown that relatively small strains are sufficient to produce dramatic changes of the polarization direction and of the energy splitting of the excitonic exchange-split doublet. Qualitatively the same results are obtained from three different kinds of QDs, consistent with a scenario involving a strain-induced anticrossing of the bright excitonic states [18]. Based on a continuum model,

which is able to reproduce the main observed features, we ascribe the effects to substantial changes of the hole states. The combination of experimental and theoretical investigations of anisotropic stress applied to QDs will allow to manipulate the excitonic characteristics in terms of anisotropy and energy in a predictable way.

We acknowledge V. Fomin, S. Kiravittaya, P. Atkinson, T. Zander, R. Trotta, G. Bester, R. Singh and C. C. Bof Bufon for fruitful discussions and technical support. V. K. and P. K. were supported by Institutional research program MSM 0021622410 and the GACR grant GA202/09/0676. This work was supported by the DFG (FOR730 and SFB 787).

- 
- [1] S. M. de Vasconcellos, S. Gordon, M. Bichler, T. Meier, and A. Zrenner, *Nature Photon.* **4**, 545 (2010).
  - [2] D. Press, T. D. Ladd, B. Zhang, and Y. Yamamoto, *Nature* **456**, 218 (2008).
  - [3] D. Brunner, B. D. Gerardot, P. A. Dalgarno, G. Wüst, K. Karrai, N. G. Stoltz, P. M. Petroff, and R. J. Warburton, *Science* **325**, 70 (2009).
  - [4] N. Akopian, N. H. Lindner, E. Poem, Y. Berlatzky, J. Avron, D. Gershoni, B. D. Gerardot, and P. M. Petroff, *Phys. Rev. Lett.* **96**, 130501 (2006).
  - [5] A. J. Hudson, R. M. Stevenson, A. J. Bennett, R. J. Young, C. A. Nicoll, P. Atkinson, K. Cooper, D. A. Ritchie, and A. J. Shields, *Phys. Rev. Lett.* **99**, 266802 (2007).
  - [6] R. Hafenbrak, S. M. Ulrich, P. Michler, L. Wang, A. Rastelli, and O. G. Schmidt, *New J. Phys.* **9** (2007).
  - [7] A. Dousse, J. Suffczynski, A. Beveratos, O. Krebs, A. Lemaitre, I. Sagnes, J. Bloch, P. Voisin, and P. Senellart, *Nature* **466**, 217 (2010).
  - [8] S. Empedocles and M. Bawendi, *Science* **278**, 2114 (1997).
  - [9] M. Bayer, G. Ortner, O. Stern, A. Kuther, A. A. Gorbunov, A. Forchel, P. Hawrylak, S. Fafard, K. Hinzer, T. L. Reinecke, et al., *Phys. Rev. B* **65**, 195315 (2002).
  - [10] B. D. Gerardot, S. Seidl, P. A. Dalgarno, R. J. Warburton, D. Granados, J. M. Garcia, K. Kowalik, O. Krebs, K. Karrai, A. Badolato, et al., *Appl. Phys. Lett.* **90**, 041101 (2007).
  - [11] M. M. Vogel, S. M. Ulrich, R. Hafenbrak, P. Michler, L. Wang, A. Rastelli, and O. G. Schmidt, *Appl. Phys. Lett.* **91** (2007).
  - [12] R. Stevenson, R. Young, P. Atkinson, K. Cooper, D. Ritchie, and A. Shields, *Nature* **439**, 179 (2006).
  - [13] I. E. Itskevich, S. G. Lyapin, I. A. Troyan, P. C. Klipstein, L. Eaves, P. C. Main, and M. Henini, *Phys. Rev. B* **58**, 4250 (1998).
  - [14] S. Seidl, M. Kroner, A. Hoge, K. Karrai, R. Warburton, A. Badolato, and P. Petroff, *Appl. Phys. Lett.* **88** (2006).
  - [15] F. Ding, R. Singh, J. D. Plumhof, T. Zander, V. Krápek, Y. H. Chen, M. Benyoucef, V. Zwiller, K. Dörr, G. Bester, et al., *Phys. Rev. Lett.* **104**, 067405 (2010).
  - [16] M. Metcalfe, S. M. Carr, A. Muller, G. S. Solomon, and J. Lawall, *Phys. Rev. Lett.* **105**, 037401 (2010).
  - [17] G. W. Bryant, M. Zieliński, N. Malkova, J. Sims, W. Jaskólski, and J. Aizpurua, *Phys. Rev. Lett.* **105**, 067404 (2010).
  - [18] R. Singh and G. Bester, *Phys. Rev. Lett.* **104**, 196803 (2010).
  - [19] D. Gammon, E. S. Snow, B. V. Shanabrook, D. S. Katzer, and D. Park, *Phys. Rev. Lett.* **76**, 3005 (1996).
  - [20] H. Y. Ramirez, C. H. Lin, C. C. Chao, Y. Hsu, W. T. You, S. Y. Huang, Y. T. Chen, H. C. Tseng, W. H. Chang, S. D. Lin, et al.,

- Phys. Rev. B **81**, 245324 (2010).
- [21] O. Benson, C. Santori, M. Pelton, and Y. Yamamoto, Phys. Rev. Lett. **84**, 2513 (2000).
  - [22] T. Zander, A. Herklotz, S. Kiravittaya, M. Benyoucef, F. Ding, P. Atkinson, S. Kumar, J. D. Plumhof, K. Dörr, A. Rastelli, et al., Opt. Express **17**, 22452 (2009).
  - [23] J. D. Plumhof, V. Křápek, L. Wang, A. Schliwa, D. Bimberg, A. Rastelli, and O. G. Schmidt, Phys. Rev. B **81**, 121309(R) (2010).
  - [24] (Supplementary materials, not submitted).
  - [25] M. D. Biegalski, K. Dörr, D. H. Kim, and H. M. Christen, Appl. Phys. Lett. **96** (2010).
  - [26] F. Ding, N. Akopian, B. Li, U. Perinetti, A. Govorov, F. M. Peeters, C. C. Bof Bufon, C. Deneke, Y. H. Chen, A. Rastelli, et al., Phys. Rev. B **82**, 075309 (2010).
  - [27] O. Stier, M. Grundmann, and D. Bimberg, Phys. Rev. B **59**, 5688 (1999).
  - [28] T. Takagahara, Phys. Rev. B **62**, 16840 (2000).
  - [29] G. E. Pikus and G. L. Bir, *Symmetry and strain induced effects in semiconductors* (Wiley, New York, 1974).